# Numerical simulation of heat transfer and hydrodynamics under transverse flow of compact bundles of tubes in shell-and-tube heat exchangers

Volodymyr Bulgakov[1]; Viktor Trokhaniak[1]; Valery Gorobets[1]; Ivan Holovach[1]; Yevhen Ihnatiev[2]; Oleksandra Trokhaniak[1]

[1]National University of Life and Environmental Sciences of Ukraine, Kyiv, Ukraine
[2]Dmytro Motornyi Tavria State Agrotechnological University, Ukraine
E-mail: vbulgakov@meta.ua

***Abstract.*** *By using the application package ANSYS Fluent, the numerical simulation of heat and mass transfer processes in the channels of shell-and-tube heat exchanger with compact placement of tube bundles has been carried out. The fields of velocities, temperatures and pressures in the heat exchanger channel were obtained and the conditions of hydrodynamic flow in the channels and the processes of heat transfer in these channels were analyzed. A new construction of shell-and-tube heat exchanger with compact arrangement of tubes in tube bundles is proposed and developed.*

***KEYWORDS****: HEAT EXCHANGER, TUBE BUNDLE, NUMERICAL SIMULATION, INTER-TUBE CHANNELS, MASS AND DIMENSIONS.*

## *1. Introduction*

Bundles of smooth cylindrical tubes with checkerboard and hallway arrangement are widely used in various heat-exchange apparatuses and devices of power installations. The review of literature sources and the results of a significant number of experimental studies of thermal-hydrodynamic characteristics of smooth tube bundles in their transverse flow [1], including studies on the heat release of checkered bundles at Reynolds numbers of $10^3 \le R_e \le 2\cdot10^5$ shows that such bundles have higher heat release compared to corridor bundles. However, they have a higher hydraulic resistance in comparison with corridor bundles.

It should be noted that surfaces of this type, used in shell-and-tube heat exchangers, lead to an increase in their mass and dimensions. One of the ways to improve these characteristics is the use of fins and heat transfer intensifiers on convective surfaces. However, the use of finned surfaces and intensifiers significantly increases the hydraulic resistance in the paths of the heat exchanger and requires the use of pumps and fans of higher power for pumping coolants. A promising direction for reducing hydraulic resistance and intensifying heat transfer on the convective surfaces of heat exchangers is the use of smooth tube bundles with a compact configuration.

Therefore, the development of new constructions of shell-and-tube heat exchangers with compact tube bundles is relevant and needs to be solved.

The aim of the research is to develop new constructions of shell-and-tube heat exchangers with compact arrangement of bundles of smooth tubes in their cross flowing by heat carriers and numerical modeling of heat and mass transfer processes in the channels of the heat exchanger.

## *2. Materials and Methods*

We consider a shell-and-tube heat exchanger with a shell of rectangular cross-section, in which bundles of tubes with a traditional staggered arrangement [1] are placed, whose pitch is 1.5×1.5 ( $s_1 / D_{outer} \cdot s_2 / D_{outer}$ ) and compact configuration in their cross-sectional flow (Fig. 1). In the heat-exchange apparatus the tubes are arranged in such a way that neighboring tubes are in contact with each other and are shifted relative to each other along the axis of ordinates by the distance K, where $\frac{0 < K < \sqrt{3}D}{2}$, and the distance $C$ corresponds to the condition $C \ge D + 5$ mm, which is caused by the fact that the technology of beam manufacturing is significantly complicated at distances between the tubes less than 5 mm.

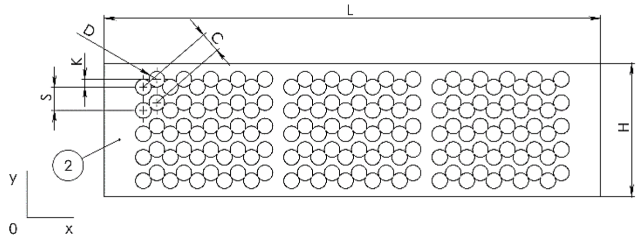


***Figure 1.*** *Tube board with compact tube arrangement (top view)*

The general view of the proposed heat exchange apparatus is schematically shown in Fig. 2.

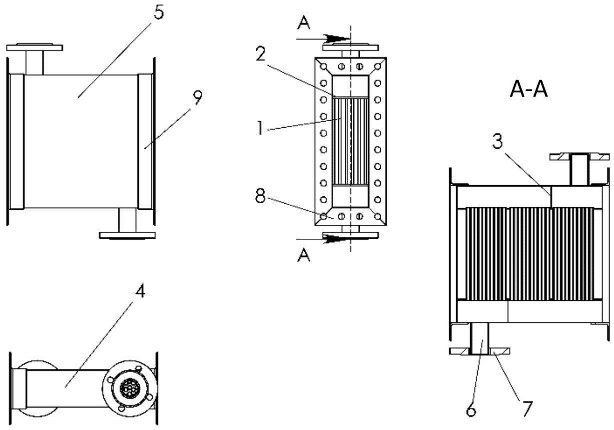


***Figure 2.*** *General view of the compact shell-and-tube heat exchanger*

Tubes in the bundle 1 are in contact with each other and shifted along the axis of ordinates at a distance $D\cdot2^{-1}$, forming a curvilinear channel. The heat-exchange apparatus consists of side walls 5 and top walls 4 with tube boards 2 fixed in it (Fig. 1), between which a vertical bundle of tubes 1 is installed. Each row of tubes in the bundle 1 has a technological gap, dividing the row into three parts, as the heat-exchange three-way device on the coolant and has a partition 3 in the upper and lower collector. The coolant inlet and outlet is provided by a flange 7 and a tube 6 (Fig. 2). The casing is a solid rigid structure and is closed from the ends by angles 8 and 9.

Numerical modeling of heat and mass transfer processes in the channels of compact configuration heat exchanger was performed using the ANSYS Fluent application software package. The mathematical model is based on the Navier-Stokes equations [2, 3] and the convective energy transfer equation. In this case the standard $k$-$\varepsilon$ model of turbulence is chosen [4, 5].

The Navier-Stokes equations describing mass transfer in the channels of the heat exchanger in 2D formulation have the form:

equation of motion:

$$\rho\left(\frac{\partial u}{\partial t}+u\frac{\partial u}{\partial x}+v\frac{\partial u}{\partial y}\right)=\frac{-\partial p}{\partial x}+\mu\left(\frac{\partial^2 u}{\partial x^2}+\frac{\partial^2 u}{\partial y^2}\right),$$
$$\rho\left(\frac{\partial v}{\partial t}+u\frac{\partial v}{\partial x}+v\frac{\partial v}{\partial y}\right)=\frac{-\partial p}{\partial y}+\mu\left(\frac{\partial^2 v}{\partial x^2}+\frac{\partial^2 v}{\partial y^2}\right), \tag{1}$$

where $\rho$ – medium density, kg·m$^{-3}$; $\mu$ − dynamic viscosity of the medium, Pa·s; $p$ – pressure, Pa; $u$, $v$, – velocity vector field, m·s$^{-1}$; $t$ – time, s.

continuity equation:

$$\frac{\partial u}{\partial x}+\frac{\partial v}{\partial y}=0. \tag{2}$$

energy conservation equation:

$$\rho C_p\left(V_x\frac{\partial T}{\partial x}+V_y\frac{\partial T}{\partial y}\right)=\frac{\partial}{\partial x}\left(\lambda\frac{\partial T}{\partial x}\right)+\frac{\partial}{\partial y}\left(\lambda\frac{\partial T}{\partial y}\right), \tag{3}$$

where $T$ – temperature at some point, °K; $\lambda$ – heat transfer coefficient of the medium, W·(m·°K)$^{-1}$; $C_p$ – specific heat capacity of the medium, J·(kg·°K)$^{-1}$.

Setting the boundary conditions (Fig. 1.) at the input:

$$x=0;\ W=W_0;\ T=T_{inlet}\ . \tag{4}$$

at the entrance:

$$x=H;\ \ \frac{\partial W}{\partial x}=0\,. \tag{5}$$

tube walls:

$$T\left(x=x_{tube_{\text{int}}}\right)\left(y=y_{tube_{\text{int}}}\right)=T_{wall_0}\ . \tag{6}$$

case walls:

$$\left|\frac{\partial T_{wall_{case}}}{\partial y}\right|_{y=0}=0\,. \tag{7}$$

conditions of adhesion on the pipe wall:

$$x=x_{tube\ \text{int}};\ y=y_{tube_{\text{int}}}\ . \tag{8}$$

sticking conditions on the enclosure wall:

$$y=H;\ W=0;\ y=0\,. \tag{9}$$

For the standard $k$-ε turbulence model, the equations are as follows:

$$\frac{\partial}{\partial t}(\rho k)+\frac{\partial}{\partial x_i}(\rho k u_i)= =\frac{\partial}{\partial x_j}\left[\left(\mu+\frac{\mu_t}{\sigma_k}\right)\frac{\partial k}{\partial x_j}\right]+G_k+G_b-\rho\varepsilon-Y_M+S_k. \tag{10}$$

and

$$\frac{\partial}{\partial t}(\rho\varepsilon)+\frac{\partial}{\partial x_i}(\rho\varepsilon u_i)= =\frac{\partial}{\partial x_j}\left[\left(\mu+\frac{\mu_t}{\sigma_\varepsilon}\right)\frac{\partial \varepsilon}{\partial x_j}\right]+C_{1\varepsilon}\frac{\varepsilon}{k}\left(G_k+C_{3\varepsilon}G_b\right)-C_{2\varepsilon}\rho\frac{\varepsilon^2}{k}+S_\varepsilon. \tag{11}$$

where $G_k$ – generation of kinetic energy turbulence due to velocity gradients; $G_b$ – generation of turbulent kinetic energy d.ue to flotation; $Y_M$ – represents the contribution of dissipation oscillation in compressible turbulence to the total dissipation rate; $C_{1\varepsilon}$, $C_{2\varepsilon}$ and $C_{3\varepsilon}$ – constants; $\sigma_k$ and $\sigma_\varepsilon$ – the turbulent Prandtl numbers for $k$ and $\varepsilon$ respectively.

For both cases the same boundary conditions are applied. Mass flow rate of air at the inlet to the heat exchangers is 0.25 kg·s$^{-1}$ with initial temperature $T_{inlet}$ = +40° C. The pipes are 200 mm high, have an outer diameter of 10 mm and a wall thickness of 1 mm. Temperature on the inside of the tubes in the first section starting from the inlet of the tube bundle is – +11.46° C, in the second and third section – +10.88° C and +10.3° C. The width of the inter-tube channel for this bundle configuration is 5 mm.

## *3. Results and discussions*

Numerical simulation results are shown in Fig. 3-7.

Fig. 3-4 shows the distribution of the temperature field and air flow rate in the heat exchanger channels with a traditional staggered arrangement. As can be seen from Fig. 3, the coolant temperature drops as it approaches the outlet of the heat exchanger. At the outlet its average value is +19° C (Fig. 3). The velocity field in the heat exchanger channels shows that the air velocity reaches 41.2 m·s$^{-1}$, near the walls at some points in the channel, and the average air velocity in the narrow cross section of the channel is about 31.1 m·s$^{-1}$ (Fig. 4).

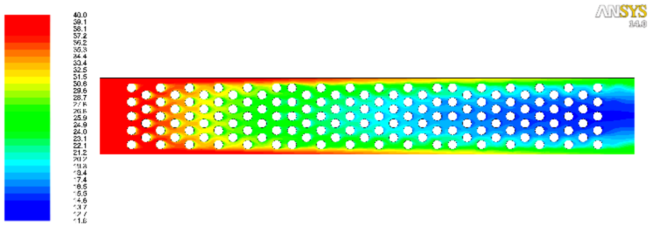

***Figure 3.*** *Temperature variation in the staggered beam channel, °C*

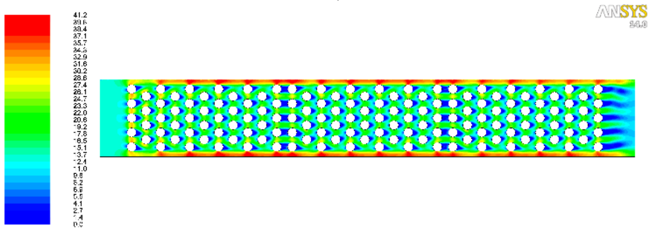

***Figure 4.*** *Air velocity in the channel of the staggered bundle, m·s$^{-1}$*

Fig. 5 shows the velocity fields in the channels of the heat exchanger with compact arrangement of the tube bundle. The analysis of the resulting velocity field shows that the maximum flow velocity values are observed at the side walls of the heat exchanger, and their values are twice as high as the velocity in the intertube channels. At some points in the channel, the air velocity reaches 85 m·s$^{-1}$, and the average air velocity in the narrow cross section of the channel is about 45 m·s$^{-1}$ (Fig. 5). In the sections of the channel separating the three sections of the tube bundle, stagnant zones take place on the last tube of each bundle. In addition, such zones are observed in the curvilinear channel sections for individual elements of the tube bundle.

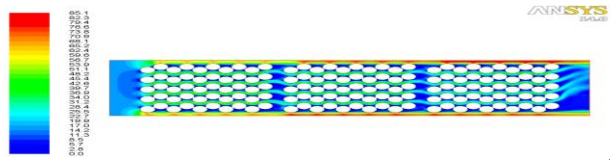

***Figure 5.*** *Air velocity in the channel of the compact beam, m·s$^{-1}$*

Fig. 6 also shows the distribution of velocity vectors in a separate tube element bundle. At the upper point of the tube, the boundary layer tears off, and there are stagnant zones at the junction of neighboring tubes. In these zones, two tear-off vortices are observed, in which the flow velocity is significantly lower than in the main flow.

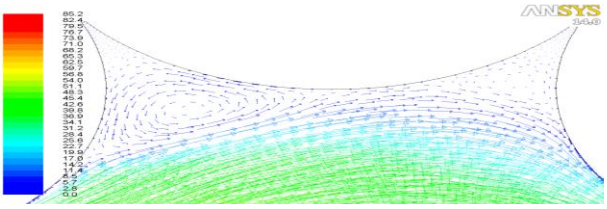

***Figure 6.*** *Velocity vector in the compact beam channel, m·s$^{-1}$*

Fig. 7 shows the distribution of the temperature field in the heat exchanger channels. As can be seen from the figure, the temperature of the coolant drops as it approaches the outlet of the heat exchanger. If at the inlet of the heat exchanger it was +40° C, then at the outlet its average value is +20.1° C. At the same time near the walls of the channel local temperature values are about +30° C.

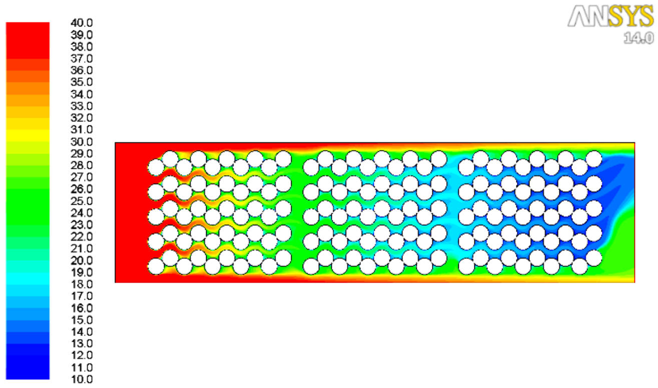


***Figure 7.*** *Temperature change in the compact beam channel, °C*

Fig. 8 shows the distribution of the pressure field in the channels of the studied heat exchanger construction. From the obtained pressure distributions it follows that the total pressure drop is about 7 kPa.

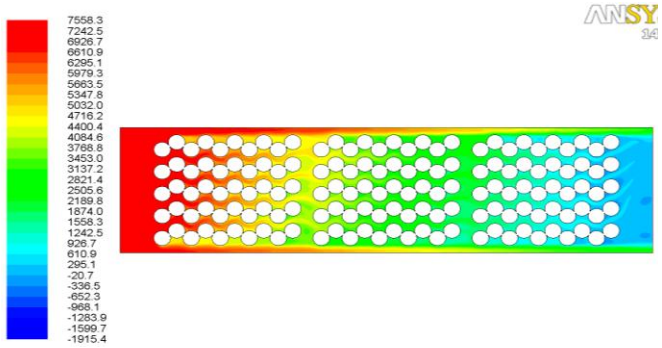


***Figure 8.*** *Pressure drop in the channel of the compact bundle, Pa*

The results of comparison of mass-dimensional parameters for the shell-and-tube heat exchanger with a staggered arrangement (1.5×1.5) and the heat exchanger of the new construction with a compact arrangement of pipes, obtained by numerical simulation, are shown in Table 1.

Table 1. Comparison of mass-dimensional characteristics of shell-and-tube heat exchanger with staggered (1.5×1.5) and compact arrangement of tube bundles.

| Main parameter of the heat exchanger | Checkerboard tube bundle | Compact tube bundle |
|---|---|---|
| Amount of heat transferred from air to water, kW | 5.20 | 5.00 |
| Air temperature at the inlet from the heat exchanger, °C | 40.0 | 40.0 |
| Air temperature at the outlet of the heat exchanger, °C | 19.3 | 20.1 |
| Mass flow rate, $kg \cdot s^{-1}$ | 0.25 | 0.25 |
| Heat transfer coefficient for air, $W \cdot m^{-2} \cdot {}^{o}K^{-1}$ | 314 | 306 |
| Differential pressure at the inlet and outlet of the heat exchanger, kPa | 3.80 | 7.00 |
| Heat exchanger length, m | 0.530 | 0.278 |
| Pipe bundle height, m | 0.20 | 0.20 |
| Number of pipes, pcs | 150 | 150 |
| Heat exchanger weight, kg | 16.6 | 15.2 |

The table shows that the input parameters of the coolant and capacity of the heat exchangers are practically the same, and the difference in the values of the heat transfer coefficients averaged over the tube surface for these constructions does not exceed 3%. The overall dimensions of the heat exchanger of the new construction are 48% less, and the weight is 10%. less compared with the traditional construction. At the same time, the value of pressure drop at the inlet and outlet, if we compare both constructions, for the proposed heat exchanger increases by 46%.

Numerical modeling makes it possible to analyze the conditions of hydrodynamic flow and heat transfer in the studied channels. As follows from the analysis of velocity, temperature and pressure fields, it is necessary to reduce the channel width between the wall and the tube row near the wall. This will reduce the flow velocity and temperature in the wall channel and increase the velocity in the main channels of the heat exchanger.

## 4. Conclusion

1. A new construction of shell-and-tube heat exchange apparatus with compact arrangement of tubes in tube bundles is proposed.
2. Numerical simulation of heat and mass transfer processes in the channels of the heat exchanger with compact arrangement of tubes using the software package ANSYS Fluent. Fields of velocities, temperatures, pressures in the studied channels are obtained.
3. The conditions of hydrodynamic flow in the channels and heat transfer processes in these channels are analyzed. Ways of improving the construction of shell-and-tube heat-exchange apparatus are proposed.
4. The comparative analysis of mass and dimensions characteristics of the known constructions of heat exchangers with the offered construction has been carried out and the decrease of dimensional parameters by 48% and mass by 10% with the same thermal capacity has been revealed.

## 5. References

1. Zhukauskas A.A., Convective heat transfer in heat exchangers, Nauka, Moscow, 1982.
2. Schlichting H., Boundary-Layer Theory, 7th edition, McGraw-Hill, New York, 1979.
3. Trokhaniak V., Klendii O. Numerical simulation of hydrodynamic and heat-mass exchange processes of a microclimate control system in an industrial greenhouse. Bulletin of the Transilvania University of Brasov, Series II: Forestry, Wood Industry, Agricultural Food Engineering, 2018, vol. 11(60), no. 2., 171-184.
4. ANSYS FLUENT Theory Guide. Release 14. ANSYS, Inc. Southpointe 275 Technology Drive Canonsburg, PA 15317, 2011
5. Bardina J.E., Huang P.G., Coakley T.J, Turbulence Modeling Validation, Testing and Development. California, NASA reports – April, 1997.